Quantum irregular scattering in the presence of a classical stability island

Petr Šeba
Nuclear Physics Institute, 250 68 Řež near Prague, Czechoslovakia
(Received 7 July 1992)

A simple irregular scattering system is investigated classically and quantum mechanically. The existence of sharp resonances due to the quantum tunneling between the chaotic and regular parts of the classical phase space is demonstrated.

PACS number(s): 05.45.+b

I. INTRODUCTION

Classical irregular scattering has been a subject of intense interest for more than one decade [1,2]. Being a typical example of transient chaos, it has attracted recently considerable attention and is a frontier of the research on classical chaotic Hamilton systems. The quantum consequences of the classical irregular scattering were studied first by Blumel and Smilansky to our knowledge [3]. They demonstrated that the existence of the classical chaotic repeller implies Ericson fluctuations of the corresponding quantum S matrix.

Today the properties of the classical and quantum irregular scattering have been investigated in various models. Their common feature was that the classical chaotic repeller (which is responsible for the appearance of the fractally organized singularities in the classical scattering) was fully hyperbolic. This means that the probability density $P(t)$ for a classical particle to stay in the interaction region for a time longer than t is given by

$$P(t) \approx e^{-\alpha t} , \tag{1}$$

with α being connected with the Lyapunov exponent of the repeller and with the corresponding Kolmogorov-Sinai entropy [4]. In the classical case it implies a self-similar structure of the scattering singularities (a kind of Cantor set). In the quantum case (1) leads to the absence of long-lived resonances and consequently to the Ericson fluctuations of the quantum cross section [3].

In the present paper we will construct a one-dimensional and time-periodic (kicked) model in which (1) is violated. Depending on the parameters of the model, the corresponding repeller will display a large stability island leading to an algebraic decay of $P(t)$:

$$P(t) \approx t^{-\alpha} . \tag{2}$$

The influence of the elliptic domain on the fractal set of the classical scattering singularities will be investigated in Sec. II. The quantum case is discussed in Sec. III, where we show that the existence of a classical island of stability leads (via tunneling) to the appearance of sharp resonances.

II. DESCRIPTION OF THE MODEL: CLASSICAL CASE

The system to be investigated consists of a one-dimensional particle moving on a line under the influence of a kicked short-range potential. The classical Hamiltonian of the model reads

$$H(p,x,t) = \tfrac{1}{2}p^2 + \lambda V(x) \sum_{n=-\infty}^{\infty} \delta(t-n) \tag{3}$$

with the potential given by

$$V(x) = -e^{-x^2} , \quad \lambda > 0 , \; x \in (-\infty, \infty) . \tag{4}$$

The dynamics of the system is governed by the classical map M,

$$p_{n+1} = p_n - V'(x_n) , \quad x_{n+1} = x_n + p_{n+1} , \tag{5}$$

where x_n and p_n denote the coordinate and the momentum, respectively, of the particle after the nth kick. Due to the short-range character of the potential we can divide the phase space into the interaction and the asymptotically free region. Under the asymptotically free region we understand that part of the phase space on which the influence of V is negligible.

Restricted on the interaction region the phase-space portrait of the above map is easily described. The origin is a fixed point of the mapping that is stable for $\lambda < 2$. It is surrounded by a set of Kolmogorov-Arnold-Moser (KAM) curves defining a stable region (the stability island) in which the motion is quasiperiodic. The stability island is imbedded into a chaotic layer that is interspersed with smaller islands [see Fig. 1(a)]. For $\lambda > 2$ the fixed point becomes unstable and the stability island disappears. Some smaller secondary island may be, however, still present. For λ large enough the interaction region becomes hyperbolic [see Fig. 1(b)].

The transport properties of the trajectories depend on the structure of the phase space. In the hyperbolic case, the probability $P(t)$ for a trajectory to stay in the interaction region is given by formula (1). It is, however, well known that the existence of a stability island changes this behavior, leading to an algebraic decay. The theoretical explanation of this fact is given in [5,6]. It has been argued that the trajectory is sticking on the boundary of this stability domain leading to $P(t) \approx t^{-\alpha}$ with α close to

1.5 [7].

During the scattering process the incoming trajectory has to pass through the interaction region to reach again the asymptotically free part of the phase space. The structure of the interaction region is therefore decisive for the structure of the scattering function [8]. Our aim is to investigate the outgoing momentum of the particle as a function of the incoming parameters. To define these quantities let us examine the classical trajectory described by the mapping (5). The evolution starts at time $t=0$ with initial conditions $(p_0, x_0)=(p_{\rm in}, x_{\rm in})$. We will assume that the initial coordinate $x_{\rm in}$ is localized in the asymptotically free domain. Due to the time periodicity of the potential we can compactify the asymptotic domain restricting $x_{\rm in}$ to an interval of a length $p_{\rm in}$. [Note that the initial conditions $(p_{\rm in}, x_{\rm in})$ and $(p_{\rm in}, x_{\rm in}+p_{\rm in})$ describe the same trajectory.] Further let (p_n, x_n) denote the trajectory at time $t=n$. Following the standard classical scattering theory we define the outgoing momentum $p_{\rm out}$ and the "outgoing" coordinate $x_{\rm out}$ by

$$\lim_{n\to\infty}(|p_n-p_{\rm out}|+|x_n-(x_{\rm out}+np_{\rm out})|)=0 \qquad (6)$$

by which the definition of $(p_{\rm in}, x_{\rm in})$ implies

$$\lim_{n\to-\infty}(|p_n-p_{\rm in}|+|x_n-(x_{\rm in}+np_{\rm in})|)=0 \ . \qquad (7)$$

The physical meaning of $x_{\rm in}$ and $x_{\rm out}$ becomes more clear if we introduce times $t_{\rm in}$ and $t_{\rm out}$ as

$$t_{\rm in}=-\frac{x_{\rm in}}{p_{\rm in}}\ , \quad t_{\rm out}=-\frac{x_{\rm out}}{p_{\rm out}}\ . \qquad (8)$$

Then

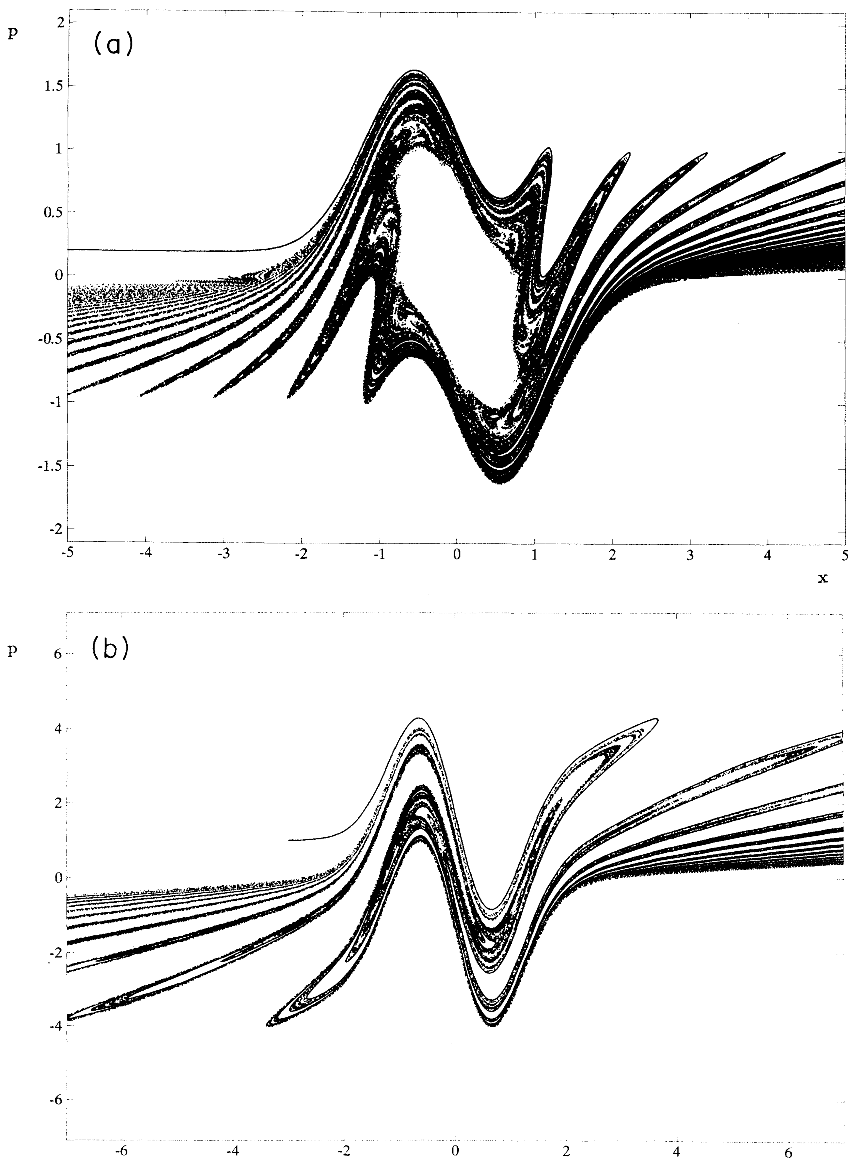

FIG. 1. (a) Phase-space portrait of the system for $\lambda=1$. (b) Phase-space portrait of the system for $\lambda=4$.

$$\Delta t = t_{\rm out} - t_{\rm in} \tag{9}$$

is nothing but the time the particle stays in the interaction region. Depending on λ the probability distribution for Δt coincides with (1) or (2).

The classical scattering describes the outgoing momentum $p_{\rm out}$ as a function of $(p_{\rm in}, x_{\rm in})$:

$$p_{\rm out} = f(p_{\rm in}, x_{\rm in}) \ . \tag{10}$$

We will fix the momentum $p_{\rm in}$ in our calculations and investigate f as a function of $x_{\rm in}$ only.

To see the intimate connection between the function f and the probability $P(t)$, let us initial trajectories with fixed $p_{\rm in}$ and with $x_{\rm in}$ being uniformly distributed in the interval $I_0 = (x_0, x_0 + p_{\rm in})$. The mapping M that propagates the initial phase-space interval $\mathcal{J} = p_{\rm in} \times I_0$ is smooth. This implies that the image $\mathcal{J}_n = M^n \mathcal{J}$ is a smooth curve in the phase space. During the time evolution some parts of the curve $\mathcal{J}_n$ may be mapped into the asymptotically free part of the phase space. The smoothness of the mapping ensures that those "asymptotically free" parts of $\mathcal{J}_n$ correspond to one or several subintervals I_n; $I_n \subset I_0$ of the initial conditions $x_{\rm in}$. The smoothness of the mapping M implies that the outgoing impulse $p_{\rm out}$ is a smooth function of $x_{\rm in}$ on I_n. The length Δ_n of initial interval which maps into the asymptotically free domain between the nth and $(n+1)$th kick is proportional to

$$\Delta_n = I_{n+1} - I_n = I_0[P(n) - P(n+1)] \ . \tag{11}$$

In the case of the exponentially decaying $P(t)$ we find

$$\begin{aligned}\Delta_n &= I_0(e^{-\alpha n} - e^{-\alpha(n+1)}) = I_0 e^{-\alpha n}(1 - e^{-\alpha}) \\ &= I(n)(1 - e^{-\alpha}) \ ,\end{aligned} \tag{12}$$

where $I(n)$ is the part of the initial interval I_0 that stays in the interaction region before $(n+1)$th kick. This means that the relative amount of trajectories leaving the interaction domain between the nth and $(n+1)$th kick is constant. Continuing the subsequent mapping of the initial interval I_0 we are left at the end with a Cantor set of initial conditions corresponding to trajectories that never escape the interaction region. (The function f describing the outgoing momentum is, of course, singular at these points). Their fractal dimension follows from (12) and is equal to [9]

$$d = \frac{\ln(2)}{\ln(2) + \alpha} \ . \tag{13}$$

For algebraic decay we find, however,

$$\Delta_n \approx \frac{\alpha}{n} I(n) \ . \tag{14}$$

The relative amount of trajectories escaping between the nth and $(n+1)$th kicks decrease with n. Lau, Finn, and Ott demonstrated [8] that the set of singular points one obtains here has a fractal dimension equal to one. The subsequent magnification of the function f will uncover a structure that is more violent on smaller scales.

In our model the influence of the elliptic island on the behavior of the scattering singularities can be easily investigated. Figures 2 and 3 show the outgoing momentum $p_{\rm out}$ as a function of $x_{\rm in}$ for two different coupling constants λ. In the first case ($\lambda = 5$) the interaction region is hyperbolic, leading to a self-similar structure of the scattering singularities. The second case corresponds to $\lambda = 0.5$ when the system displays a large stability island. The difference in the structure of the singular points is clearly visible.

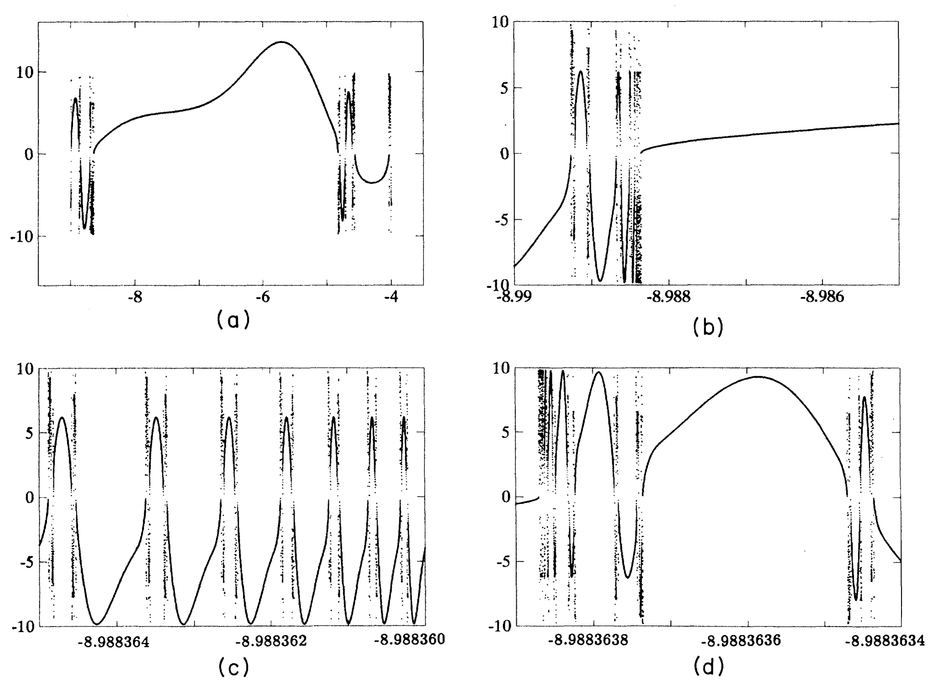

FIG. 2. $p_{\rm out}$ as a function of $x_{\rm in}$ in a series of subsequently magnified plots, for $\lambda = 5$. The interaction region is hyperbolic, and the structure of the scattering singularities is self-similar.

III. THE QUANTUM CASE

Before describing the quantum case it is reasonable to reformulate the scattering in a time-independent frame. In the classical mechanics this can be achieved by adding the time as a new canonical variable into the phase space. The conjugated momentum is then given by $\mathcal{E}$ and the new Hamiltonian reads

$$K(p,x,\mathcal{E},t)=\mathcal{E}+H(p,x,t) , \tag{15}$$

where $H(p,x,t)$ is the original time-dependent Hamiltonian (3). Since we deal with a time-periodic model we will assume the new coordinate t to be periodic and confined to an interval $t\in[0,1]$. The extended phase space is therefore equivalent to a four-dimensional cylinder. Introducing a formal new time τ, the classical equations of motion in the extended phase space read

$$\begin{aligned} \frac{dx}{d\tau}&=\frac{\partial K}{\partial p} , \quad \frac{dp}{d\tau}=-\frac{\partial K}{\partial x} , \\ \frac{dt}{d\tau}&=\frac{\partial K}{\partial \mathcal{E}}=1 , \quad \frac{d\mathcal{E}}{d\tau}=-\frac{\partial K}{\partial t}=-\frac{\partial H}{\partial t} , \end{aligned} \tag{16}$$

and are, of course, fully equivalent to the original Hamilton equations.

In the quantum case a formal quantization of (15) leads to a Floquet Hamiltonian K introduced by Howland [10] and Yajima [11],

$$K=i\hbar\frac{\partial}{\partial t}+H(t) , \tag{17}$$

which is defined on an extended Hilbert space $\mathcal{H}=L^2((0,1)\times\mathbb{R})$ with periodic boundary conditions with respect to the variable t. (For the properties of the Floquet Hamiltonian in kicked systems see [13].)

Knowing K and the corresponding free Floquet Hamiltonian K_0,

$$K_0=i\hbar\frac{\partial}{\partial t}-\frac{\hbar^2}{2}\frac{\partial^2}{\partial x^2} , \tag{18}$$

we can define the evolution operators $U(\tau)$ and $U_0(\tau)$,

$$i\hbar\frac{\partial}{\partial\tau}U(\tau)=KU(\tau) , \quad i\hbar\frac{\partial}{\partial\tau}U_0(\tau)=K_0U_0(\tau) . \tag{19}$$

The quantum S matrix is then given by

$$S=\Omega_-^*\Omega_+ , \tag{20}$$

with Ω_- and Ω_+ being the wave operators

$$\begin{aligned} \Omega_+&=s\lim_{\tau\to-\infty} U(-\tau)U_0(\tau) , \\ \Omega_-&=s\lim_{\tau\to\infty} U(-\tau)U_0(\tau) . \end{aligned} \tag{21}$$

The S matrix (20) describes the quantum scattering and can be investigated using the methods of the *standard stationary scattering theory.* Let us now discuss some of its properties.

From the definition (20) it follows that the free Floquet Hamiltonian K_0 commutes with S:

$$[S,K_0]=0 . \tag{22}$$

This in turn means that the free quasienergy (i.e., the eigenenergy of the operator K_0) is conserved during the scattering process. This fact has several consequences. One of them is that the particle can gain only a discrete amount of energy. This can be seen easily if we realize that the free Floquet Hamiltonian K_0 separates and defines in such a way the incoming and outgoing "channels" for the quantum scattering. The free wave function f_n belonging to the nth channel with quasienergy Θ (i.e., solving the equation $K_0f_n=\Theta f_n$) has the form

$$f_n(x,t)=e^{i2\pi nt}(a_ne^{(i/\hbar)p_nx}+b_ne^{-(i/\hbar)p_nx}) \tag{23}$$

with p_n being the momentum of the particle

$$\tfrac{1}{2}p_n^2+2\pi\hbar n=\Theta . \tag{24}$$

Let us assume that the incoming particle has quasienergy Θ and momentum equal to p_{in}. After the scattering we will find the particle with a momentum p_{out}. Due to the quasienergy conservation, p_{in} and p_{out} have to fulfill

$$\tfrac{1}{2}p_{\text{in}}^2+2\pi\hbar n_{\text{in}}=\tfrac{1}{2}p_{\text{out}}^2+2\pi\hbar n_{\text{out}} , \tag{25}$$

with n_{in} and n_{out} being integers. Hence the kinetic energy $E=p^2/2$ of the particle can change only by discrete portions of $2\pi\hbar$.

The conservation of the quasienergy enables us to decompose the S matrix as

$$S=\int S(\Theta)d\Theta , \tag{26}$$

where $S(\Theta)$ is the on-shell S matrix referring to the scattering with a given quasienergy Θ. We will show later that using $S(\Theta)$ one can naturally define the dynamic resonances as poles of $S(\Theta)$ when continuing the S matrix into the complex quasienergy plane.

Concerning the S matrix several questions arise. The first and most important one is to what extend the S matrix $S(\Theta)$ reflects the phase-space structure of the classical model. Using the four-dimensional reformulation of the classical mechanics one can write $S(\Theta)$ in its semiclassical form. The classical trajectories required for the semiclassical quantization of S are obtained as follows: At $\tau\to-\infty$ and $|x|\to\infty$ the generalized momentum $\mathcal{E}$ is set to $\mathcal{E}_{\text{in}}$ while the momentum p_{in} of the incoming particle is taken to give the quasienergy Θ its specified value:

$$\mathcal{E}_{\text{in}}+\tfrac{1}{2}p_{\text{in}}^2=\Theta . \tag{27}$$

Now the initial coordinate x_{in} is chosen and the equations of motion (16) are solved. As $\tau\to\infty$ the momentum $\mathcal{E}$ becomes $\mathcal{E}_{\text{out}}$

$$\mathcal{E}_{\text{out}}=f(x_{\text{in}},\mathcal{E}_{\text{in}}) \tag{28}$$

and the outgoing momentum p_{out} fulfills

$$\Theta=\mathcal{E}_{\text{out}}+\tfrac{1}{2}p_{\text{out}}^2 . \tag{29}$$

Each trajectory s that satisfies $f(x_{\text{in}},\mathcal{E}_{\text{in}})=\mathcal{E}_{\text{out}}$ contributes to the transition probability $\mathcal{E}_{\text{in}}\to\mathcal{E}_{\text{out}}$ a term

$$P^{(s)}_{\mathcal{E}_{\rm in}\to\mathcal{E}_{\rm out}}=\left[\frac{\partial f(x_{\rm in},\mathcal{E}_{\rm in})}{\partial x_{\rm in}}\right]^{-1}_{(s)} . \tag{30}$$

The quantum S matrix $S(\Theta)$ is then obtained using the method of Maslov as explained by Miller [12] and applied by Blumel and Smilansky [3]. For this reason we introduce the reduced classical action

$$I(s)=\int_{(s)}p\,dx+\int_{(s)}\mathcal{E}\,dt-p_{\rm out}x_{\rm out}-\mathcal{E}_{\rm out}t_{\rm out}+p_{\rm in}x_{\rm in}+\mathcal{E}_{\rm in}t_{\rm in} . \tag{31}$$

This choice of the action ensures that $I(s)$ does not depend on the initial and final points along the trajectory as long as they stay in the asymptotic (interaction-free) region.

In the semiclassical theory the "generalized momentum" $\mathcal{E}$ is quantized as

$$\mathcal{E}_n=2\pi\hbar n\ ,\quad n\in Z \tag{32}$$

and the semiclassical S matrix is equal to

$$S_{n,m}(\Theta)=S_{\mathcal{E}_n,\mathcal{E}_m}(\Theta)=\sum_{(s)}[P^{(s)}_{\mathcal{E}_n\to\mathcal{E}_m}]^{1/2}\exp\left[i\frac{I(s)}{\hbar}-\frac{1}{2}i\pi\alpha(s)\right] , \tag{33}$$

where $\alpha(s)$ is the Maslov index of the trajectory s. The summation in expression (33) runs over all classical trajectories s connecting $\mathcal{E}_n$ and $\mathcal{E}_m$. In the time-independent case formula (33) has been used by Blumel and Smilansky to evaluate the correlation function $A_{n,m}(\varepsilon)$ of the S matrix $S(\Theta)$:

$$A_{n,m}(\varepsilon)=\langle S^*_{n,m}(\Theta)S_{n,m}(\Theta+\varepsilon)\rangle_\Theta , \tag{34}$$

where $\langle\ \rangle_\Theta$ denotes the average about a classically small quasienergy interval $\Delta\Theta$. Inserting (33) into (34) and decomposing the final expression with respect to ε, Blumel and Smilansky showed that in the time-independent case the exponential decrease of the classical probability (1) implies the absence of long-lived resonances in the quantum case and correspondingly Ericson fluctuations [3]. Using the same method we find

$$A_{n,m}=\left\langle\sum_{(s)}P^{(s)}_{\mathcal{E}_n\to\mathcal{E}_m}(\Theta)\exp\left[i\varepsilon\frac{1}{\hbar}\frac{\partial I(s)}{\partial\Theta}\right]\right\rangle_\Theta+o(\varepsilon) . \tag{35}$$

The derivative of the action $I(s)$ with respect to the quasienergy Θ is equal to the formal "time" τ the particle spends in the interaction region. From the classical equations of motion (16) we learn, however, that $\tau=t$ plus some constant that can be set to zero. Therefore $\partial I/\partial\Theta$ is equal to the true time delay ΔT. Labeling the trajectories with ΔT we can rewrite (35) as

$$A_{n,m}\approx\int\langle P_{\mathcal{E}_n\to\mathcal{E}_m}(\Theta,\Delta T)\rangle_\Theta e^{i(\varepsilon/\hbar)T}d(\Delta T) , \tag{36}$$

where $P_{\mathcal{E}_n\to\mathcal{E}_m}(\Theta,\Delta T)$ is the classical conditional probability that a transition $\mathcal{E}_n\to\mathcal{E}_m$ takes place with a trajectory staying in the interaction region for a time ΔT. Replacing $P_{\mathcal{E}_n\to\mathcal{E}_m}(\Theta,\Delta T)$ with (1) we find [3]

$$A_{n,m}(\varepsilon)\approx A_{n,m}(0)\frac{\alpha}{\alpha-i\dfrac{\varepsilon}{\hbar}} . \tag{37}$$

The fluctuations of the S matrix are therefore here also of the Ericson type [14] (see Fig. 4).

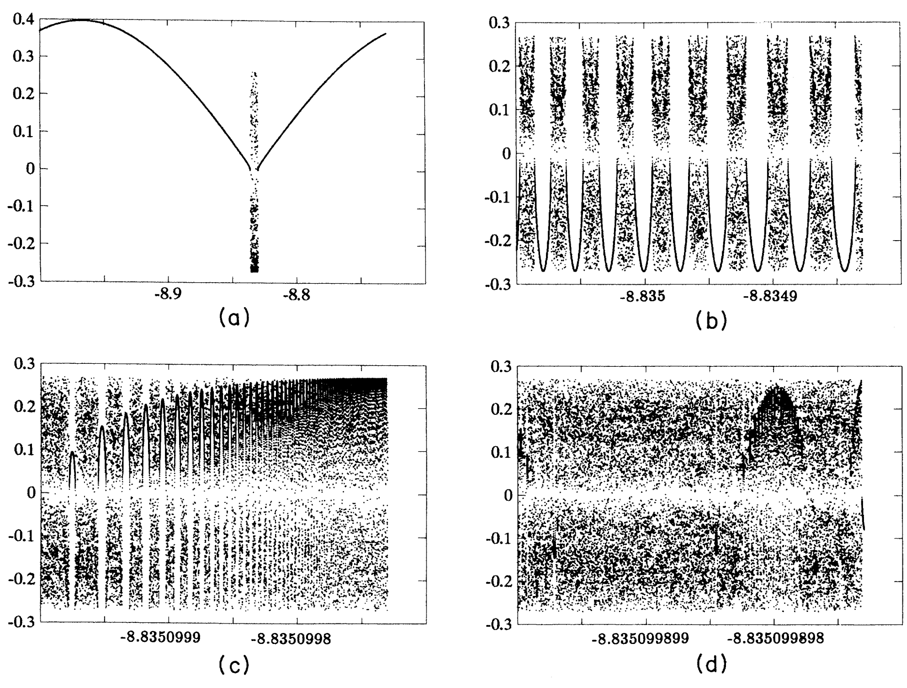

FIG. 3. Same as in Fig. 2, but for $\lambda=0.5$. The structure of the scattering singularities is not self-similar. The plot indicates a fractal with fractal dimension equal to 1.

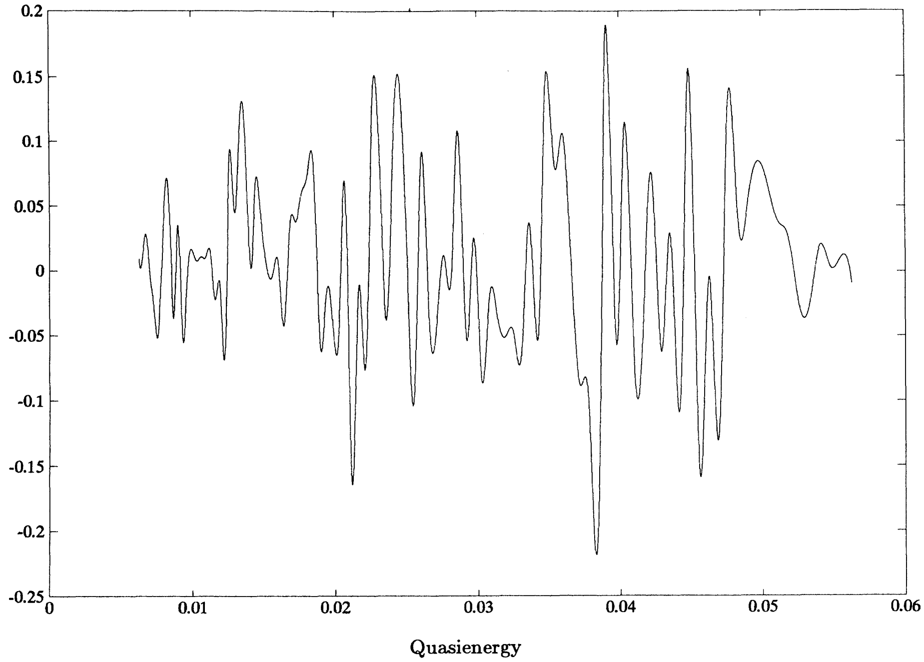

FIG. 4. Fluctuations of the real part of the matrix element $S_{1,1}$ for $\lambda=5$ and $\hbar=0.05$.

The situation changes, however, if the interaction region contains a well-developed stability island. The decay becomes algebraic (2), and (37) is not applicable. Instead of Ericson fluctuations, the numerical calculations uncover here a series of sharp resonance peaks that can be understood as appearing due to the quantum tunneling into the stability island (see Fig. 5).

To gain some insight into the resonance formation we followed numerically the evolution of the quantum wave packet evaluating simultaneously the corresponding Husimi distribution ρ_H [15]:

$$\rho_H(p,q)=|\langle \varphi_{p,q}|\Psi\rangle|^2 \tag{38}$$

with $\varphi_{p,q}$ being the minimal wave packet

$$\varphi_{p,q}(x)=\frac{1}{(\pi\hbar)^{1/2}}\exp\left[\frac{i}{\hbar}px-\frac{(x-q)^2}{2\hbar}\right]. \tag{39}$$

At time $t=0$ the wave packet was localized in the asymptotically free domain having an initial momentum equal to p_{in}. The state then was propagated using a quantum map associated with the Hamiltonian (3) and the corre-

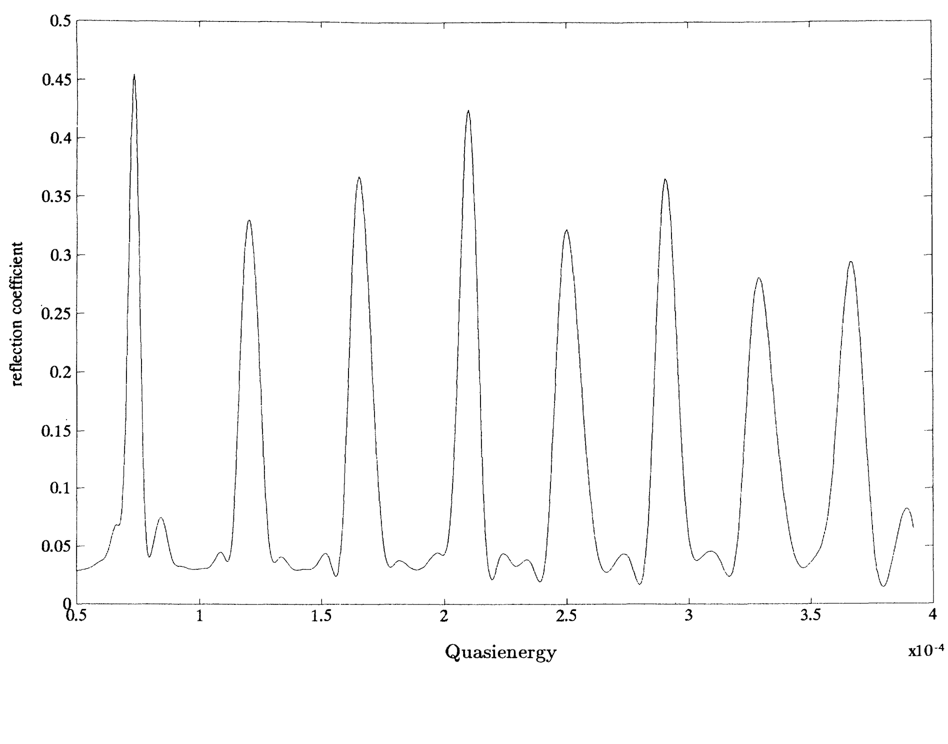

FIG. 5. The absolute value of the matrix element $S_{1,1}$ as a function of the quasienergy evaluated for $\lambda=0.5$ and $\hbar=0.01$. The sharp resonance peaks can be understood as appearing due to the quantum tunneling into the stability island.

sponding Husimi distribution was evaluated. The results for the resonance quasienergy are plotted on Fig. 6. A similar plot has been evaluated also for a nonresonant quasienergy and plotted in Fig. 7. The process of the resonance trapping of the wave packet in the classical stability region is clearly apparent. In the nonresonant case the wave packet goes "through" the interaction region without displaying a substantial influence of stability island.

The Husimi distribution of the wave function trapped in the stability domain is displayed in Fig. 8 and compared with the classical case. This figure demonstrates that the main part of the wave function is actually trapped in the stability domain.

A very important structure of the Floquet Hamiltonian is the Brillouin-zone structure of its spectrum. From the solution of the eigenvalue equation

$$Kf_{\Theta}(x,t)=\Theta f_{\Theta}(x,t) \tag{40}$$

one immediately obtains a whole class of further solutions $f_{\Theta+2\pi\hbar n}$:

$$f_{\Theta+2\pi\hbar n}(x,t)=f_{\Theta}(x,t)e^{i2\pi nt} . \tag{41}$$

Obviously the first Brillouin zone $0<\Theta<2\pi\hbar$ contains the whole relevant physical information. This is why we can restrict ourselves to the quasienergy interval $\Theta\in[0,2\pi\hbar)$ when scanning for the resonance peaks. To demonstrate the connection between the quantum resonances and the classical stability island we will suppose for a moment that the outermost KAM curve, which sets the boundary of the island and is impenetrable for the classical particle, is impenetrable for quantum particles as well. Then some quantum states will be trapped inside the island, leading to eigenvalues imbedded into the continuous spectrum of the Floquet Hamiltonian K. [Formally these eigenvalues are real poles of the S matrix $S(\Theta)$.]

The number $\mathcal{N}$ of them is given roughly by the area $\mathcal{S}$ of the stability island divided by $2\pi\hbar$:

$$\mathcal{N}\approx\frac{\mathcal{S}}{2\pi\hbar} . \tag{42}$$

Moreover, in the semiclassical regime the eigenvalues are nearly equidistant. (This is a direct consequence of the EBK quantization; see, for instance, [16].) The distance Δ between the neighboring eigenvalues is easily approximated by

$$\Delta\approx\frac{2\pi\hbar}{\mathcal{N}} . \tag{43}$$

Inserting (42) into (43) we find

$$\Delta\approx\frac{4\pi^2}{\mathcal{S}}\hbar^2 . \tag{44}$$

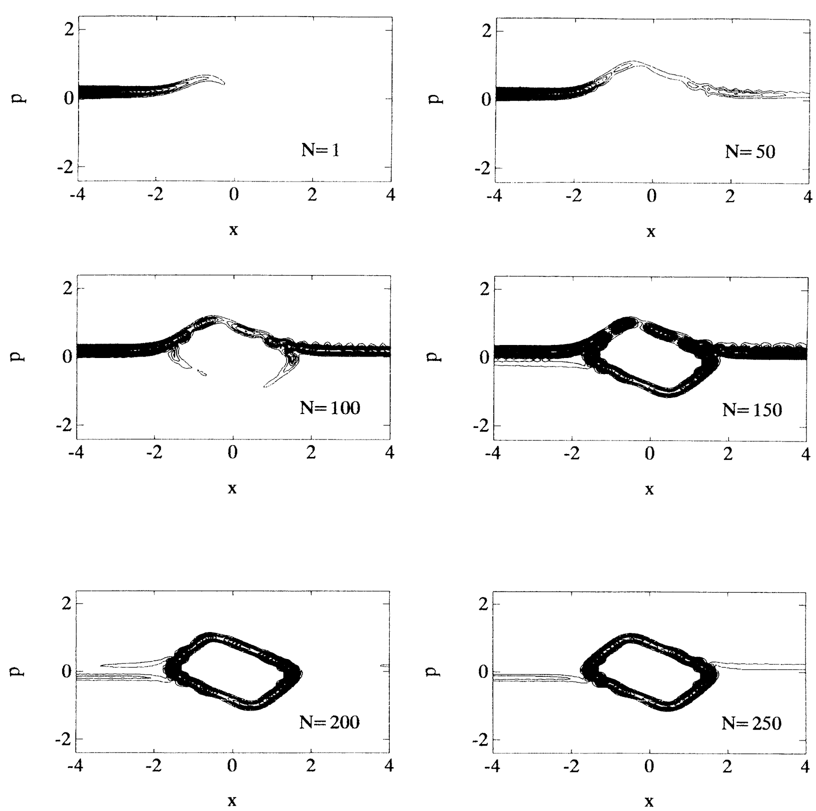

FIG. 6. The time evolution of the Husimi distribution evaluated for a resonant quasienergy. The trapping of the wave function in the stability island is clearly visible. The number of kicks is indicated inside the figures.

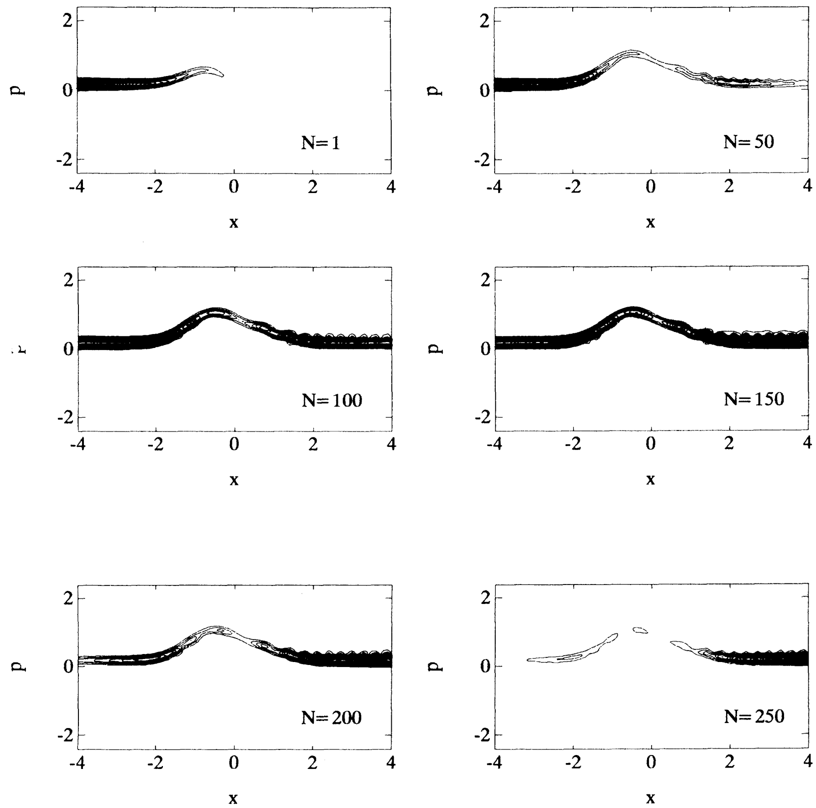

FIG. 7. Same as in Fig. 6, but for a nonresonant quasienergy. There is no trapping inside the stability domain.

The quantum tunneling through the outermost KAM curve turns the eigenvalues into resonances and the poles on the S matrix $S(\Theta)$ will move from the real axis. One can find them, however, by continuing $S(\Theta)$ into the complex plane. The real part of the resonance poles will remain nearly equal to the above-described eigenvalues (assuming the tunneling is not very strong). As a result we have to find (for small $\hbar$) a ladder of nearly equidistant resonance peaks when plotting the quantum transition probabilities as a function of the quasienergy (see Fig. 5). The formula (44) suggests a quadratic dependence of the mean distance Δ on $\hbar$. We evaluated Δ for several $\hbar$ and

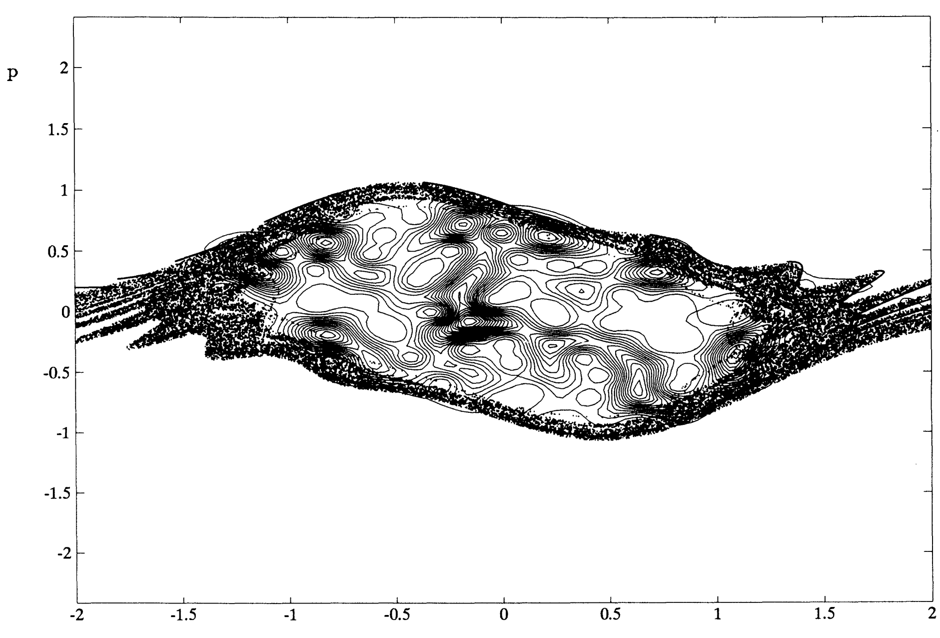

FIG. 8. The Husimi distribution of the wave function trapped in the stability domain is displayed and compared with the corresponding classical phase-space portrait.

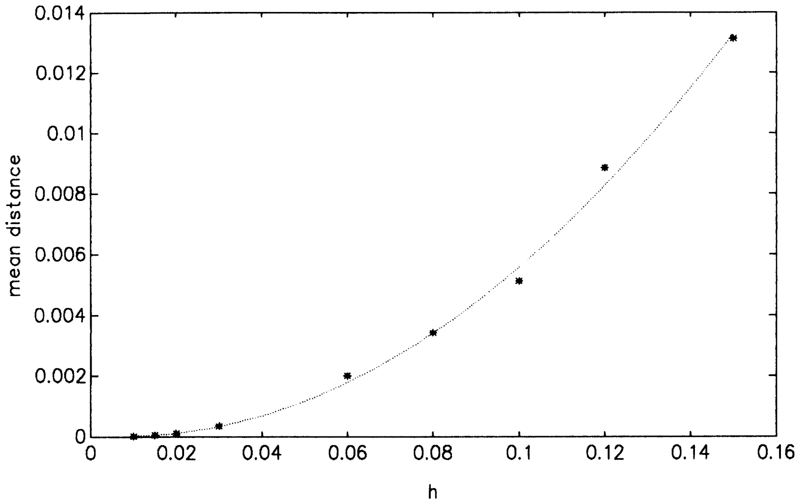

FIG. 9. The mean distance between the resonance peaks as a function of $\hbar$ (asterisks) compared with the prediction of the formula (44).

compared the result with the prediction of (44) in Fig. 9. The agreement is astonishingly good.

IV. CONCLUSION

We have investigated the scattering in a one-dimensional time-periodic model. The results show that the existence of a well-developed stability island leads in the classical mechanics to a fat fractal of scattering singularities. In the quantum case the tunneling into the stability island leads to the appearance of sharp resonances. It is tempting to speculate that the same mechanism will create resonances also in other scattering systems with well-developed stability islands.

[1] B. Eckhard and C. Jung, J. Phys. A **19**, L829 (1986).
[2] T. Tel, J. Phys. A **22**, L691 (1989).
[3] R. Blumel and U. Smilansky, Phys. Rev. Lett. **60**, 477 (1988); **64**, 241 (1991).
[4] Ch. Jung and T. Tel, J. Phys. A **24**, 2793 (1991).
[5] Ch. F. F. Karney, Physica **8D**, 360 (1983).
[6] J. D. Meis and E. Ott, Phys. Rev. Lett. **55**, 2741 (1985).
[7] B. V. Chirikov and D. L. Shepelyanski, Physica **13D**, 394 (1984).
[8] Y. T. Lau, J. M. Finn, and E. Ott, Phys. Rev. Lett. **66**, 978 (1991).
[9] T. Viczek, *Fractal Growth Phenomena* (World Scientific, Singapore, 1989).
[10] J. Howland, Ind. J. Math. **28**, 471 (1979).
[11] K. Yajima, J. Math. Soc. Jpn. **29**, 729 (1977).
[12] W. H. Miller, Adv. Chem. Phys. **30**, 77 (1975).
[13] T. Ericson, Ann. Phys. (N.Y.) **23**, 390 (1963).
[14] G. Karner, V. I. Manko, and L. Streit, University of Bielefeld Report No. BiBoS399/89 (unpublished).
[15] K. Takashima, Prog. Theor. Phys. Suppl. **27**, 558 (1983).
[16] L. D. Landau and E. M. Lifsitz, *Quantum Mechanics* (Pergamon, Oxford, 1965), Chap. 48.